



14th IEA Heat Pump Conference
15-18 May 2023, Chicago, Illinois

Experimental Investigation Into The Effect of Charge Optimization And Standard Test Conditions On The Seasonal Performance In An R410A Heat Pump With Dedicated Subcooler

Sugun Tej Inampudi^a, Stefan Elbel^{a,b*}

^aUniversity of Illinois at Urbana-Champaign, Department of Mechanical Science and Engineering, Air Conditioning and Refrigeration Center, 1206 West Green Street, Urbana, IL 61801, USA

^bCreative Thermal Solutions, Inc., 2209 North Willow Road, Urbana, IL, 61802, USA

Abstract

There is an increased focus on the amount of refrigerant charge used in the HVAC&R systems due to the new restrictions and ongoing phase down of high GWP refrigerants as part of the F-gas regulation. In the current study, seasonal performance for a variable speed compressor in an R410A water ethylene glycol (WEG) heat pump system having a nominal heating capacity of 9 kW is estimated according to EU 14825. This study experimentally studied the effect of charge and the fixed/variable outlet condition on the seasonal performance of the water heat pump equipped with a variable speed compressor. The results of a charge optimization done at part load conditions show an unexpected peak in COP_{dec} and results indicates that optimum charge has a higher impact on the efficiency at part load conditions than the nominal conditions. Based on the experimental results, the difference in the order of 5% in $SCOP$ is found when comparing optimum charge and non-optimum charge in a variable speed compressor. $SCOP$ can change by almost 22% depending on whether fixed/variable condenser temperature outlet operation is used.

© HPC2023.

Selection and/or peer-review under the responsibility of the organizers of the 14th IEA Heat Pump Conference 2023.

Keywords: charge optimization; heat pump; seasonal performance; dedicated subcooler; EU 14825; SCOP

1. Introduction

Due to the new restrictions and ongoing phase down of high GWP refrigerants as part of the F-gas regulation, there is an increased focus on the amount of refrigerant used in the HVAC&R systems. This increases the focus on potential benefits of having the optimum charge in a HVAC&R system. There are experimental studies which show the impact of charge level on cooling/heating capacity and energy efficiency. A refrigerant charge reduction of 25% led to an average energy efficiency reduction of about 15% and capacity degradation of about 20%. When the refrigerant was charged to 75% of design, the SEER value decreased by 16% [1]. An experimental investigation was conducted to study the effect of low charge level of R-22 on the performance of a 3-ton residential air conditioning system. The experimental results show that if a system is undercharged to 90% there is only a 3.5% reduction in cooling capacity however, the system performance suffers serious degradation if the level of charge drops below 80% [2].

Though there are many studies which predict that not operating at the optimum refrigerant charge can impact the cooling capacity and the efficiency of the system. The charge optimization is done at the nominal operating conditions and this charge might not be the optimum for part load operations. Beginning 2023, there are new DOE requirements for the HVAC systems to have higher SEER in USA. This increases the focus on seasonal performance than a single point efficiency. One of the ways to increase the seasonal performance is to use compressor capacity modulation.

* Corresponding author. Tel.: +1-217-721-9621.
E-mail address: elbel@illinois.edu.

An experimental study by the same authors analysed the effect of charge on the *COP* of a single speed and variable speed compressor in a dedicated subcooler chiller system. A peak was observed in *COP* at charge before the receiver starts filling up and this peak was more pronounced at the part load conditions. When the variable speed compressor was tested at a lower charge, the IPLV.SI was higher by 5% than when tested with the higher charge. They concluded that the peak in *COP* occurs due to the relative sizing of the condenser and subcooler and the optimum charge corresponds to the scenario when some portion of the two-phase heat transfer is happening in the subcooler [3]. Additionally, cases with different high side configuration were discussed and the peak *COP* was only observed for the case with a dedicated subcooler [4].

In the current study, the seasonal performance of an R410A heat pump for water heating application with a variable speed compressor is estimated according to EU 14825 standard [5]. The seasonal performance is estimated for the case with constant and variable $T_{w,co,out}$. The initial tests are done using the nominal charge of 1.5 kg which was estimated for the same R410A system for cooling application [3,4]. The charge optimization for the heat pump is conducted at part load conditions to see if a peak in *COP* like the cooling application is observed [3,4]. This study also tries to explain a peak in *COP* observed in this dedicated subcooler with receiver system when the receiver is empty during the charge optimization test. The variable speed compressor is then tested at the optimum charge with constant and variable $T_{w,co,out}$ to determine the effect of charge optimization on seasonal performance estimation.

2. Experimental Facility Description

Figure 1 shows the schematic of the R410A Water Ethylene Glycol (WEG) heat pump. A mixture of 20 % water and ethylene glycol is used as the secondary fluid. Two closed WEG loops are connected to the evaporator and condenser. Variable speed pumps and electric heaters are used to control the WEG flow rate and the outlet temperature of the condenser and the inlet temperature of the evaporator. An additional heat exchanger with chilled water flowing through is included in the condenser WEG loop to reject the heat from the condenser WEG loop. All the heat exchangers used in the facility are brazed plate heat exchangers (BPHX) and their dimensions are provided in Table 1. A 0.9 L receiver is connected between the condenser and the subcooler. Superheat is maintained at constant value by an electronic expansion valve (EXV) equipped with a superheat controller while the subcooling is a function of the charge.

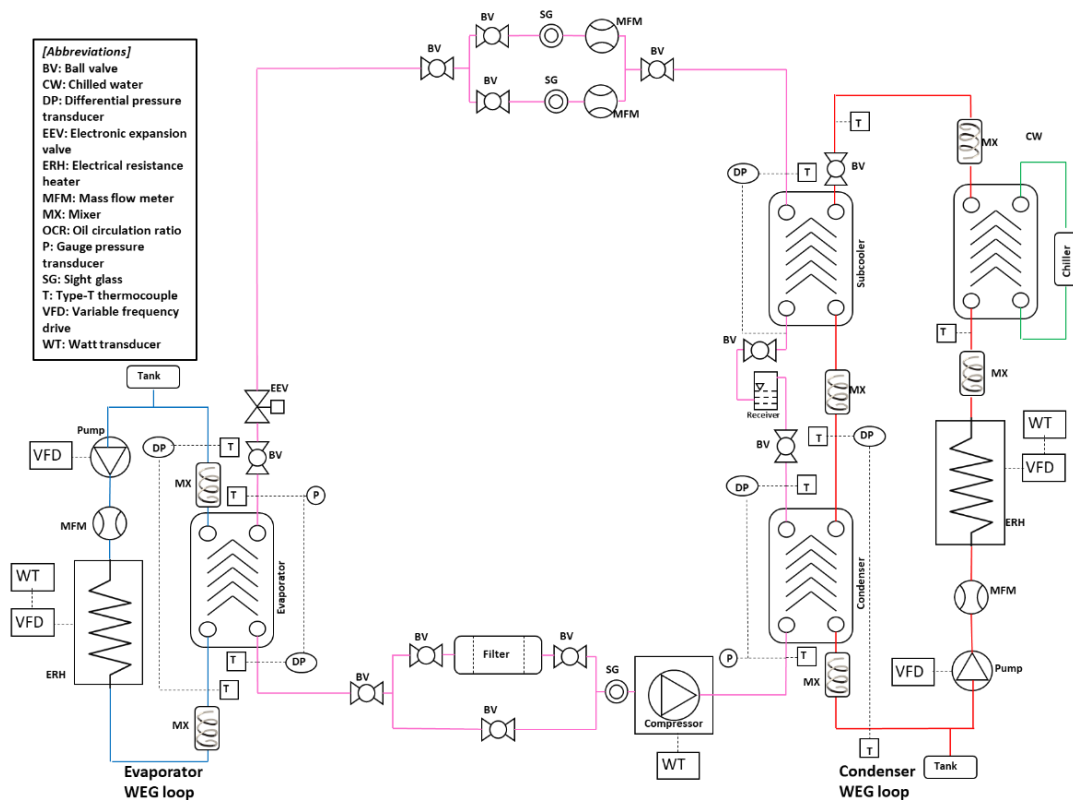


Fig. 1. Schematic of the R410A experimental facility

This experimental facility was also used by the same authors to compare the seasonal performance of different compressor modulation strategies for cooling application and the results show that variable speed compressor has the best seasonal performance [6,7,8]. A variable speed compressor than can operate between 15 and 100 Hz is used for this study.

Type-T thermocouples, absolute and differential pressure transducers, and Coriolis-type mass flow meters are used to obtain the refrigerant side measurements while type-T thermocouples, differential pressure transducers, and Coriolis-type mass flow meters are used to obtain WEG measurements. The data is collected at steady-state conditions at 5s intervals for 15 consecutive minutes, and the data is averaged over the collection period. REFPROP 10.0 was used to calculate the WEG and R410A properties [9]. The uncertainty of the sensors used in the experimental facility is presented in Table 2. This estimation does not include the uncertainty in thermophysical properties. However, the uncertainty in enthalpy difference can be approximated as the uncertainty in specific heat which is around $\pm 0.5\%$ [9]. An uncertainty propagation analysis carried out revealed an experimental uncertainty of $\pm 0.3\%$ for $\dot{Q}_{co+sc,ref}$ and $\pm 5.7\%$ for $\dot{Q}_{co+sc,WEG}$.

Table 1 Dimensions of the BPHX

Heat exchanger	Length (mm)	Width (mm)	Number of plates
Evaporator	311	111	28
Condenser	311	111	14
Subcooler	207	77	14

Table 2 Summary of the measured and calculated uncertainties

Instrument	Thermocouple (°C)	Pressure transducer (kPa)	Mass flow meter (g/s)	Wattmeter (kW)	$\dot{Q}_{co+sc,avg}$ (kW)	$COP_{dec,avg}$ (-)	$COP_{dec,weg}$ (-)
Uncertainty	± 0.2	$\pm 0.2\%$	$\pm 0.2\%$	$\pm 0.5\%$	$\pm 3.0\%$	$\pm 3.1\%$	$\pm 5.8\%$

The capacity is calculated on the refrigerant side and the WEG side. For the WEG side, mass flow rate, temperature, and specific heat are used to calculate capacity as shown in Equation (1). For the refrigerant side, temperature and pressure are used to calculate the enthalpy which is then used with the mass flow rate to calculate the capacity as shown in Equation (2). The capacity reported is the average of the refrigerant side and WEG side capacity given by Equation (3). The difference between the two capacities is indicated by the error given by Equation (4). This error is always less than 6% for the part load rating tests. Power consumed by the compressor is measured using a Wattmeter. The ratio of the average capacity and power consumed by the compressor is used to calculate the $COP_{dec,avg}$ as shown in Equation (5). The heating capacity is always the combined heat rejected from the condenser and dedicated subcooler.

$$\dot{Q}_{co+sc,weg} = \dot{m}_{WEG} c_p \Delta T \quad (1)$$

$$\dot{Q}_{co+sc,ref} = \dot{m}_{ref} \Delta h \quad (2)$$

$$\dot{Q}_{co+sc,avg} = \frac{(\dot{Q}_{co+sc,WEG} + \dot{Q}_{co+sc,ref})}{2} \quad (3)$$

$$\varepsilon_{\dot{Q}_{co+sc}} = \frac{(\dot{Q}_{co+sc,avg} - \dot{Q}_{co+sc,WEG}) \cdot 100}{\dot{Q}_{co+sc,avg}} \quad (4)$$

$$COP_{dec,avg} = \dot{Q}_{co+sc,avg} / \dot{W}_{cp} \quad (5)$$

$\dot{Q}_{co+sc,avg}$ as defined in Equation (3) and $COP_{dec,avg}$ are used for the estimation of the seasonal performance of the compressor (Sections 4.1, 4.3 and 4.4), but $\dot{Q}_{co+sc,weg}$ defined in Equation (1) and $COP_{dec,weg}$ are used during the charge optimization sections (Section 4.2). When the system is undercharged, the refrigerant is a two phase substance at the subcooler outlet which affects the Coriolis mass flow meter measurement. Though this problem does not exist at higher refrigerant charges, $\dot{Q}_{co+sc,weg}$ and $COP_{dec,weg}$ are still used to be consistent across all the refrigerant charges tested.

3. EU 14825 Standard

EU 14825 standard is used for the determination of the seasonal performance of a water heat pump [5]. Though there is an USA standard AHRI 551/591 available for chiller application, there is no such standard for water heat pump [10]. This standard defines the seasonal performance using $SCOP$, seasonal coefficient of performance. $SCOP$ is a representative for the whole designated heating season calculated as the reference annual heating demand divided by the annual electricity consumption for heating. Only the compressor power consumption (W_{cp}) is included in the estimation of $SCOP$. The current study estimates the seasonal performance using part load conditions for water/brine-to-water units for low temperature application for average heating season. These test conditions are given in Table 3. $SCOP$ is calculated using COP_{PL} , outside temperature, number of annual hours in which these temperatures are recorded. EU 14825 standard defines these characteristic reference temperatures and annual hours. The methodology to determine the $SCOP$ according the European standard EN 14825 was explained for a domestic brine-to-water heat pump for low-temperature application in another study [11].

Table 3 Part load conditions for water/brine-to-water units for low temperature application for average heating season

Test point	Part load ratio (%)	Outdoor (Evaporator) BPHX temperature [°C]	Indoor (Condenser) BPHX fixed outlet [°C]	Indoor (Condenser) BPHX fixed outlet [°C]
E&F	100	10/7	30/35	30/35
A	88	10/*	*/35	*/34
B	54	10/*	*/35	*/30
C	35	10/*	*/35	*/27
D	15	10/*	*/35	*/24

In this study, the bivalent temperature was selected equal to the design temperature causing the E and F conditions to become the same. As seen in Table 3, condenser and evaporator inlet and outlet conditions are mentioned for the full load condition (E&F) while for the remaining part load conditions, only the condenser outlet and evaporator inlet temperatures are given. The standard requires that the condenser and evaporator WEG flow rate used for the full load condition be used for the remaining part load conditions as well. The standard requires the evaporator outlet WEG temperature to be 7°C for the 100% load condition but the WEG flow required to achieve a 3°C temperature difference across the evaporator is beyond the maximum flow rate possible with the available pumps in the experimental facility. Hence, a 5°C temperature difference is used for the evaporator as well. A 5°C is used for the condenser in the EU 14825 standard as well as for the evaporator in cooling application in both the USA and EU standard [5,10].

If the compressor cannot be unloaded to the required part load ratio, then the compressor is run at the minimum step of unloading at the same condenser outlet and evaporator inlet condition shown in Table 3 and COP_{dec} is calculated. Then this COP_{dec} is degraded to COP_{PL} using the CR , $C_d = 0.9$ as shown in Equations (6) and (7). CR is the ratio of the required heating demand to the supplied heating capacity by the system. The degradation coefficient C_d can be determined by performing a specific cycling loss test defined in EU 14825 or a value of 0.9 can be assumed according to the standard [5].

$$CR = \frac{\dot{Q}_{load}}{\dot{Q}_{capacity}} \quad (6)$$

$$COP_{PL} = COP_{dec} \frac{CR}{C_d \cdot CR + (1 - C_d)} \quad (7)$$

4. Results And Discussion

4.1. Seasonal performance of a variable speed compressor with 1.5 kg of charge

4.1.1. Constant condenser WEG inlet conditions

Seasonal performance results of a variable speed compressor charged with 1.5 kg of refrigerant are shown in Figure 2. The selected compressor can operate between 15 and 100 Hz. The load is a linear function of the part load conditions. The maximum heating capacity is equal to the load at the E&F condition obtained with the variable speed compressor operating at 72.5 Hz. This operating frequency is equal to the one used for the

cooling performance tests conducted [8]. As the test condition changes from E&F to D, the condenser WEG inlet temperature remains constant at 35°C and the required load changes from 100% to 15%. The variable speed compressor can match the required heating load at E&F, A and B condition by changing the compressor operating frequency. Since this compressor can operate below 28.3 Hz, it should have been able to match the required heating load at C condition. Additionally, at the D condition, the compressor should have been able to operate at 15 Hz (lowest possible frequency) and provide a closer heating capacity. However, if the compressor operates at a frequency below 28.3 Hz, the required pressure ratio is outside the compressor operating envelop and thus it is limited to this 28.3 Hz. This high pressure ratio is caused by the constant condenser outlet test condition on WEG side. The compressor undergoes cycling losses at C and D condition and the magnitude of these losses are higher at the D condition. This can be by the difference between $COP_{dec,avg}$ and COP_{PL} and the cycling losses in Figure 2. $SCOP_{avg}$ calculated for this compressor is 4.33.

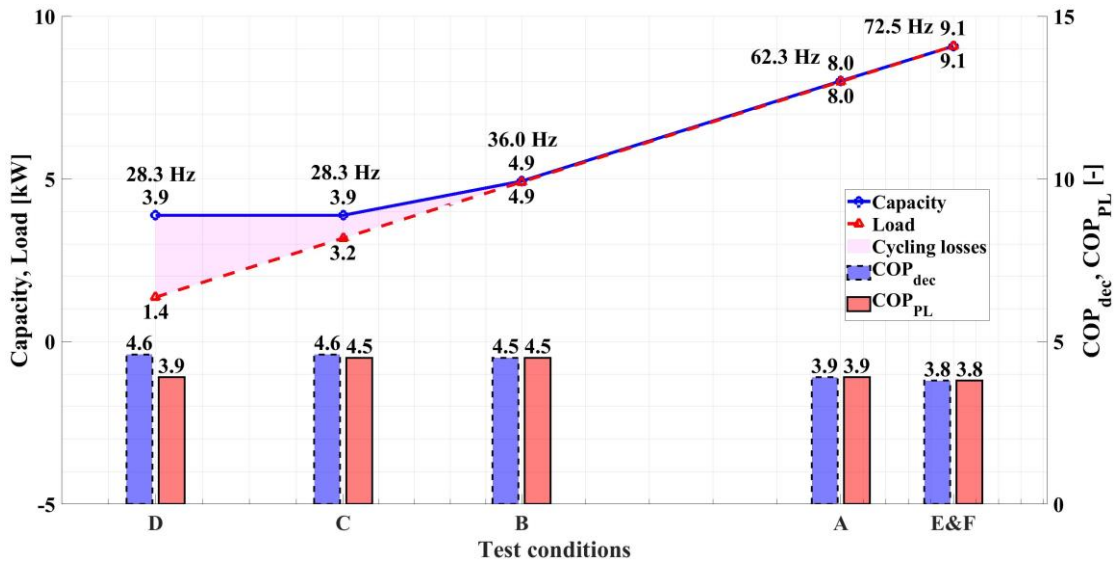


Fig. 2. Seasonal performance of variable speed compressor with constant $T_{weg,co,out}$

4.1.2. Variable condenser WEG outlet temperature

Seasonal performance results of the same variable speed compressor when tested according to the variable condenser WEG outlet temperature requirements are shown in Figure 3.

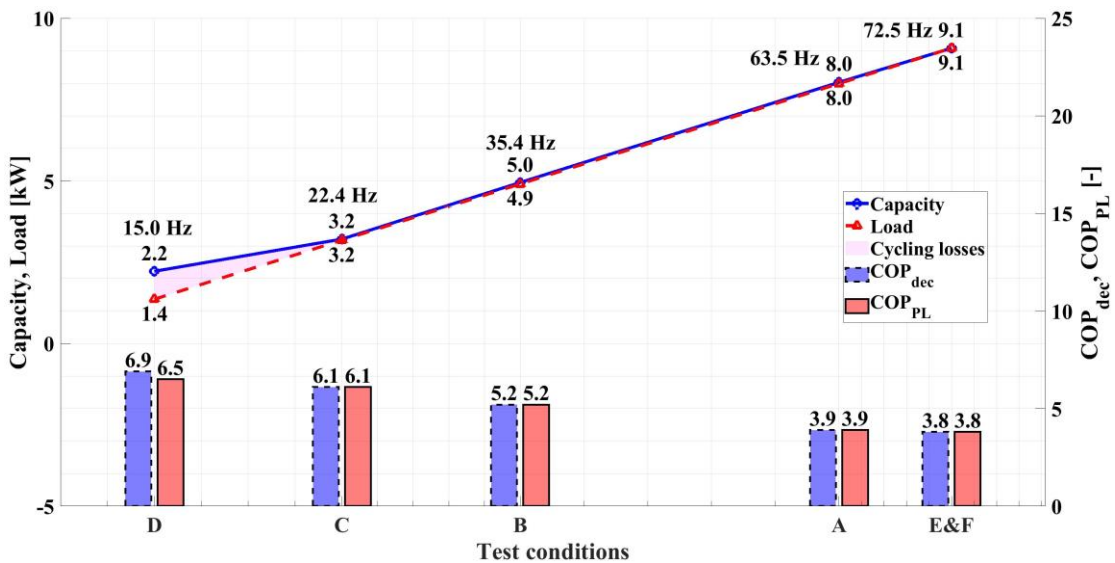


Fig. 3. Seasonal performance of variable speed compressor with variable $T_{weg,co,out}$

The operating frequency and the performance of the compressor are the same at E&F condition due to the similarities between both the standard requirements. However, at the part load test conditions, the required part load ratio remains the same as the case with constant WEG outlet temperature but the condenser outlet temperature changes. This temperature drops from 35°C at E&F condition to 24°C at D condition. This drop in the condenser temperature causes the pressure ratio to be within the compressor operating envelop. Thus, the compressor can match the required cooling load at C condition and operate at its lowest possible frequency of 15 Hz at D condition. This lowers the cycling losses experienced by the compressor and both $COP_{dec,avg}$ and $COP_{PL,avg}$ are higher when using this test matrix. The $SCOP_{avg}$ calculated for this compressor is 5.26.

4.2. Charge optimization of variable speed compressor at B condition

Charge optimization results of the variable speed compressor at B condition are shown in Figures 4, 5 and Table 4. Figure 4 shows the variation of $COP_{dec,weg}$, $\dot{Q}_{co+sc,weg}$ with charge while Figure 5 shows the variation of compressor work, superheat and subcooling with charge.

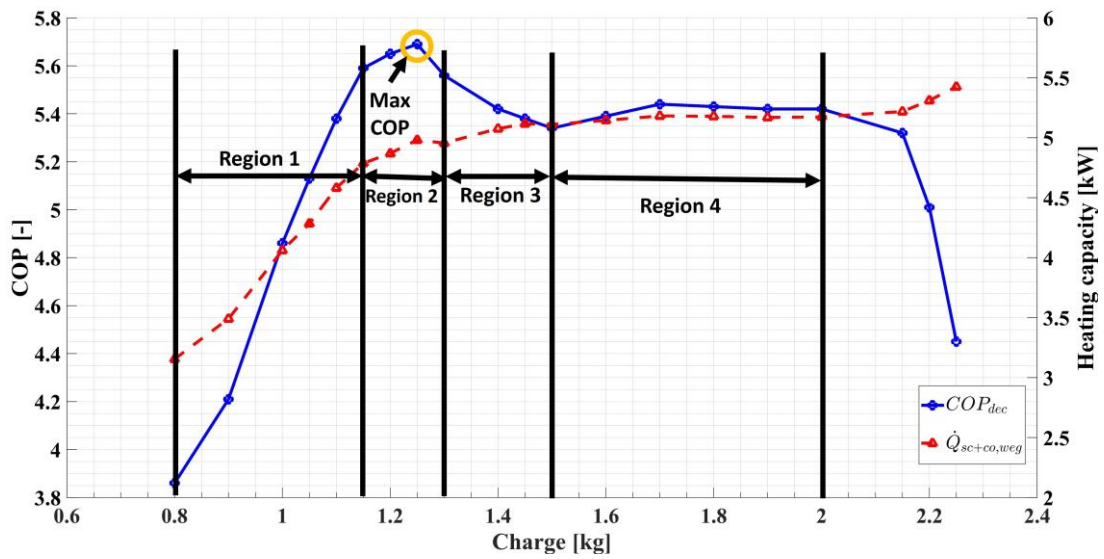


Fig. 4. Variation of $COP_{dec,weg}$ and $\dot{Q}_{co+sc,weg}$ of variable speed compressor with charge at B condition

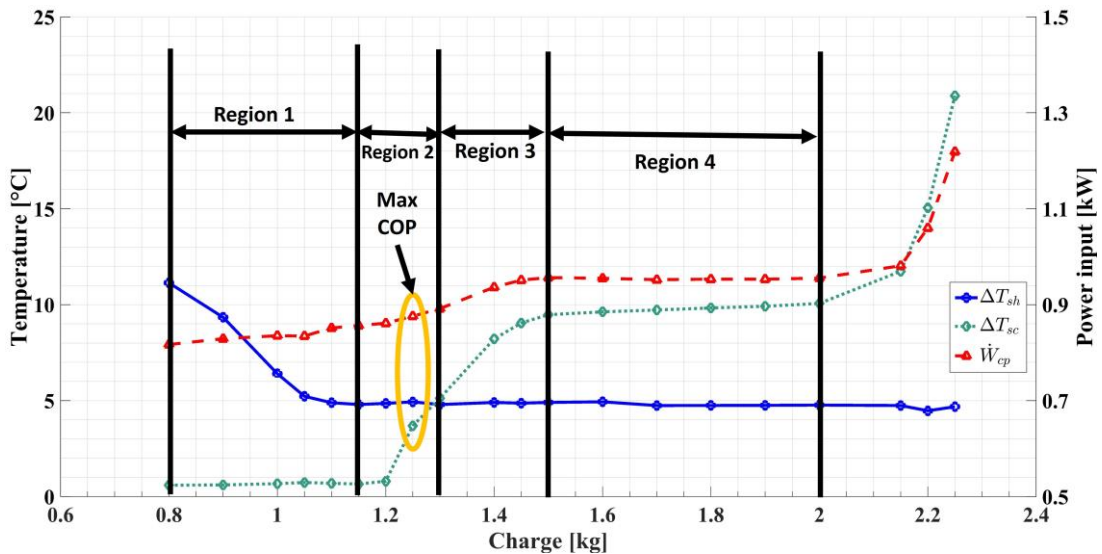


Fig. 5. Variation of W_{cp} , ΔT_{sh} and ΔT_{sc} of variable speed compressor with charge at B condition

Table 4 presents the charge, $COP_{dec,weg}$, percentage change in the heating capacity, power consumption between two consecutive refrigerant charges. It also shows the difference between the subcooler outlet enthalpy of two consecutive charges. The evaporator superheat and UA are also available in Table 4. Though Figure 4 looks like a typical charge optimization curve for a system with TXV/EXV with a receiver, there is an unexpected peak in $COP_{dec,weg}$ that occurs when the receiver is empty. To explain the reason why there is a peak in $COP_{dec,weg}$ and why it occurs at that charge, the entire charge optimization curves are divided into four regions.

Region 1 (0.80 to 1.15 kg): In this region, the refrigerant charge added goes to the evaporator due to the EXV being completely open. Thus, as the charge increases in the evaporator, the superheat at the evaporator outlet reduces. This in turn increases the evaporator UA. A lower superheat, higher evaporator UA increases the heat transfer in the evaporator and thus also increases the condenser heat rejection. Additionally, the subcooler outlet enthalpy increases in this region. Thus, there is no positive impact of the subcooler in this region. At the end of this region, the evaporator superheat reaches a constant value and the EXV can maintain the required superheat.

Region 2 (1.20 to 1.25 kg): The maximum $COP_{dec,weg}$ occurs in this region. The increase in the heating capacity at this point compared to the previous charge is due to the decrease in subcooler outlet enthalpy. This is the first point where the subcooler outlet enthalpy reduces compared to the previous charge. The compressor power also increases; however, the percentage increase of the heating capacity is higher than the percentage increase of power consumption. Thus, this results in a peak in $COP_{dec,weg}$. This is the last point in region 2 and 3 where the relation in Equation (8) is valid.

$$\frac{\Delta\dot{Q}_{co}}{\dot{Q}_{co}} > \frac{\Delta\dot{W}_{cp}}{\dot{W}_{cp}} \quad (8)$$

Table 4 Variation of different parameters with charge for a variable speed compressor at B condition

Charge [kg]	$COP_{dec,weg}$ [-]	$\Delta\dot{Q}_{co}/\dot{Q}_{co}$ [%]	$\Delta\dot{W}_{cp}/\dot{W}_{cp}$ [%]	$\frac{\Delta\dot{Q}_{co}/\dot{Q}_{co} - \Delta\dot{W}_{cp}/\dot{W}_{cp}}{\dot{Q}_{co}}$ [%]	ΔT_{sh} [°C]	UA_{ev} [kW/°C]	Δh_{scro} [kJ/kg]
0.80	3.86	-	-	-	11.1	0.34	
0.90	4.21	+10.65	+1.49	+9.16	9.3	0.44	+1.13
1.00	4.86	+16.35	+0.75	+15.59	6.4	0.72	+1.56
1.05	5.13	+5.48	-0.09	+5.57	5.2	0.83	+0.15
1.10	5.38	+6.94	+2.02	+4.92	4.9	0.72	+1.06
1.15	5.59	+4.48	+0.60	+3.88	4.8	0.70	+0.41
1.20	5.65	+1.73	+0.57	+1.17	4.9	0.70	-0.05
1.25	5.69	+2.29	+1.71	+0.58	4.9	0.71	-4.27
1.30	5.56	-0.52	+1.79	-2.31	4.8	0.71	-1.65
1.40	5.42	+2.43	+5.01	-2.58	4.9	0.72	-2.17
1.45	5.38	+0.79	+1.58	-0.79	4.9	0.73	-0.37
1.50	5.34	-0.10	+0.54	-0.64	4.9	0.72	-0.41
1.60	5.39	+0.66	-0.15	+0.81	4.9	0.72	-0.24
1.70	5.44	+0.72	-0.30	+1.02	4.7	0.74	-0.14
1.80	5.43	-0.07	0.12	-0.19	4.7	0.74	-0.32
1.90	5.42	-0.17	-0.02	-0.15	4.8	0.74	-0.07
2.00	5.42	+0.09	0.25	-0.16	4.8	0.74	0.03
2.15	5.32	+0.86	2.69	-1.83	4.7	0.74	-1.14
2.20	5.01	+1.77	8.01	-6.24	4.5	0.75	-0.79
2.25	4.45	+2.16	15.02	-12.86	4.7	0.74	-0.66

Quality at the subcooler inlet, ratio of heat transfer happening in the subcooler to the total heat transfer happening in the condenser and subcooler and the single phase (subcooled liquid) heat transfer happening in the subcooler are plotted against the charge in Figure 6. In the region 1, the quality at the subcooler inlet

increases because as the charge is added to the system, refrigerant mass flow rate increases while the heat transfer happening in the condenser does not change significantly. This causes an increase in the quality at the subcooler inlet (condenser outlet). The $COP_{dec,weq}$ maximum occurs when the quality at the subcooler inlet is 34%. This means at the charge corresponding to the $COP_{dec,weq}$ peak, some portion of the two phase heat transfer happens in the subcooler. This can also be seen that 30% of the total heat transfer is happening in the subcooler at the maximum $COP_{dec,weq}$ charge and as the charge increases, more heat transfer occurs in the condenser. Additionally, the single phase heat transfer happening in the subcooler increases as the charge increases beyond the maximum $COP_{dec,weq}$ charge but the ratio of heat transfer happening in subcooler decreases. This indicates that as additional charge is added though the single phase heat transfer increases in the subcooler, the total heat transfer happening in the subcooler decreases.

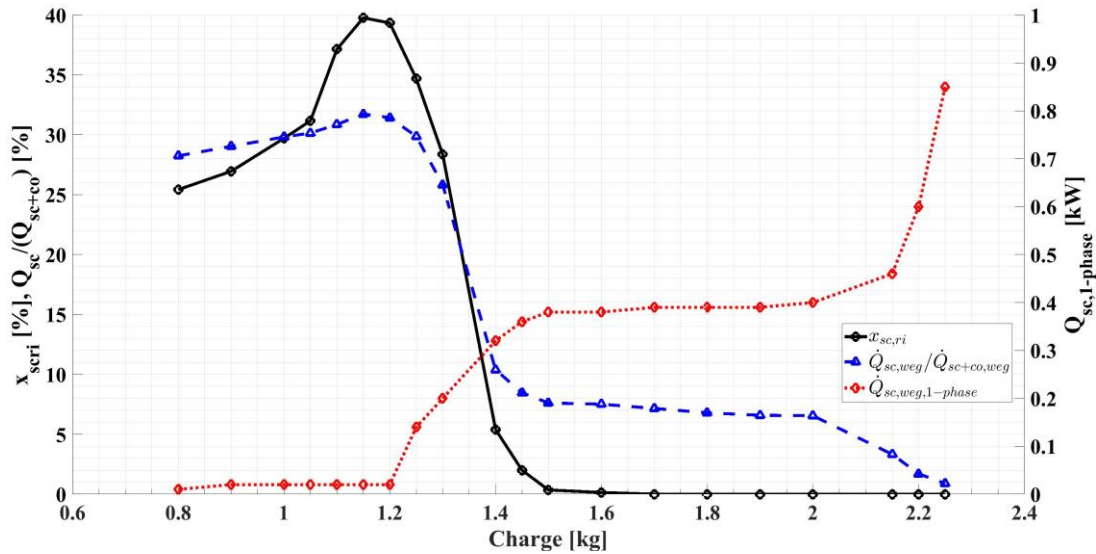


Fig. 6. Variation of refrigerant quality at subcooler inlet, subcooler heat transfer with charge

The maximum $COP_{dec,weq}$ approximately corresponds to a configuration shown in Figure 7 which indicates that the single phase subcooled refrigerant exists only at the outlet of the subcooler.

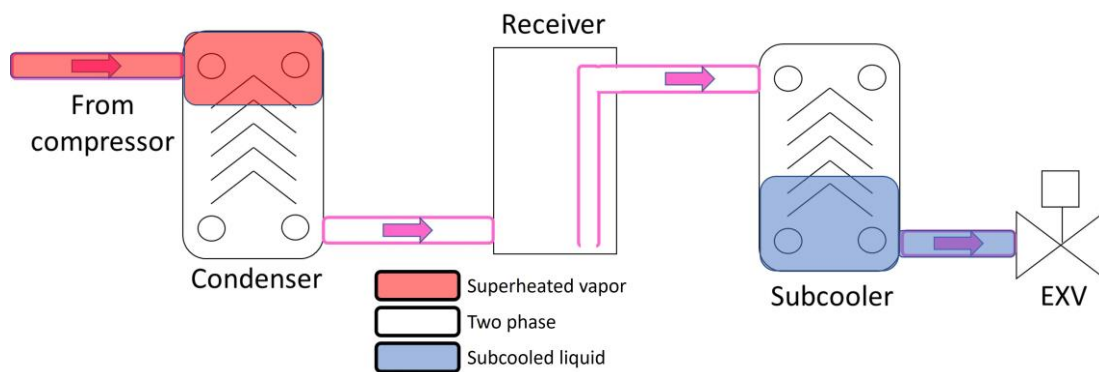


Fig. 7. Approximate distribution of the refrigerant at the maximum COP_{dec} charge

Region 3 (1.30 to 1.50 kg): In this region, the relative increase in compressor power consumption is higher than the relative increase in heating capacity and the relation shown in Equation (9) is valid. Though the amount of subcooling increases 5°C to 9.4°C as shown in Figure 5, the enthalpy at the subcooler outlet only drops by 2.9 kJ/kg in the entire region 3. This drop is lower than the drop of 4.3 kJ/kg observed from the 1.20 kg to the peak $COP_{dec,weq}$ charge of 1.25 kg. As the charge increases in this region, the condensation pressure goes up and the subcooling at the subcooler outlet increase, the heating capacity is determined by the enthalpy at the subcooler outlet not the subcooling. Additionally, there is a limit on the heating capacity due to the minimum

possible subcooler outlet enthalpy determined the inlet temperature of WEG while there is no such limit on the compressor outlet enthalpy and compressor power consumption.

$$\frac{\Delta\dot{Q}_{co}}{\dot{Q}_{co}} < \frac{\Delta W_{cp}}{W_{cp}} \quad (9)$$

At the maximum $COP_{dec,weg}$ charge and in region 3, the subcooler inlet is two phase refrigerant. As the charge increases in region 3, the fraction of two phase heat transfer happening the subcooler reduces. This reduction is seen by the drop in the subcooler inlet refrigerant quality in Figure 6. This increases the amount of two phase heat transfer happening in the condenser. Therefore, to get a higher heat transfer rate in the same condenser area, the temperature difference across the refrigerant and WEG in the condenser must increase. This leads to a higher condensation pressure and subcooling at the subcooler outlet. The increase in power consumption due to this higher condensation pressure is more than the increase in heating capacity as shown in Equation (9), causing a drop in the $COP_{dec,weg}$ in region 3.

Region 4 (1.60 to 2.00 kg) and beyond (2.15 to 2.25 kg): Region 4 starts when the receiver starts filling up with the liquid refrigerant. The additional refrigerant charge gets accumulated in the receiver and thus there is no change in the system performance. When the charge is increased beyond the region 4 and the receiver holding capacity, the additional charge gets accumulated in the condenser which increases the condensation pressure, power consumption and reduces the $COP_{dec,weg}$.

4.3. Seasonal performance of a variable speed compressor with 1.25 kg of charge

The results of the charge optimization study reveal that a peak in $COP_{dec,avg}$ is seen when the system operates at 1.25 kg. To understand the impact of the charge optimization on the seasonal performance ($SCOP_{avg}$), the variable speed compressor is now tested using constant and variable condenser WEG inlet with 1.25 kg of refrigerant charge.

4.3.1. Constant condenser WEG inlet conditions

Seasonal performance results of a variable speed compressor charged with 1.25 kg of refrigerant are shown in Figure 8. The operating frequencies of the compressor are the same as in Section 4.1.1. However, the heating capacities with the reduced refrigerant charge is lower at the full load conditions by 2.2% than the one available when operating with 1.5 kg of charge. This difference in heating capacity drops at the part load conditions. The $COP_{dec,avg}$ is higher for the 1.25 kg compared to 1.5 kg charge. The $COP_{dec,avg}$ is 2% higher at the full load condition while it 4.3% higher at C&D and 6.6% at B condition. This shows that the charge optimization has a higher impact at the part load conditions than the full load conditions.

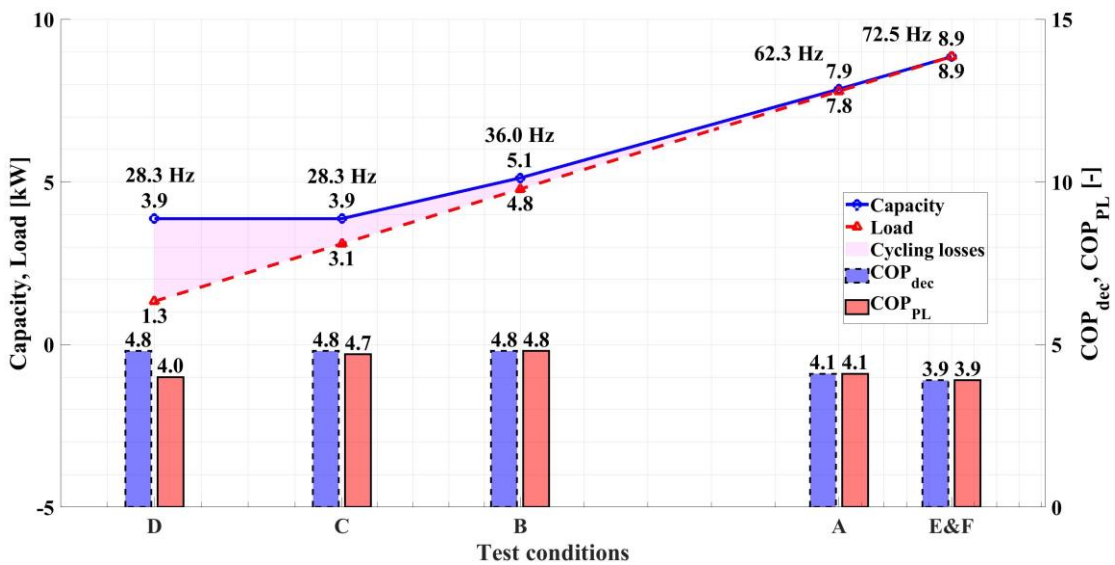


Fig. 8. Seasonal performance of variable speed compressor with constant $T_{weg,co,out}$

Though it can be seen from Figure 8 that the compressor undergoes cycling losses at B condition, no cycling losses were included and $COP_{PL,avg}$ is equal to $COP_{dec,avg}$. The compressor can match the required heating capacity at B condition by operating at a frequency lower than 36.0 Hz, it is still operated at 36.0 Hz to match the frequency used when operating with 1.5 kg. This frequency allows an estimation of the effect of only charge on $COP_{dec,avg}$ for both the cases. And to ensure the case with 1.25 kg is not penalized for this operation, cycling losses are not included. The compressor does undergo cycling losses at C and D conditions for this lower refrigerant charge as well. However, the $COP_{PL,avg}$ are still higher for the lower refrigerant case. The $SCOP_{avg}$ for this compressor at 1.25 kg refrigerant charge is 4.56.

4.3.2. Variable condenser outlet temperature

Seasonal performance is estimated for the variable speed compressor charged with 1.25 kg of refrigerant according to the variable $T_{weg,co,out}$ test matrix. The results of the seasonal performance test are shown in Figure 9. The heating capacity at the full load condition (E&F) is still lower by 2% than when operating with 1.5 kg of refrigerant charge. The operating frequency of the compressor is maintained the same as the test case with higher refrigerant charge to only include the effect of refrigerant charge on the seasonal performance. The $COP_{dec,avg}$ and $COP_{PL,avg}$ are higher with 1.25 kg for all the test conditions and the difference is higher at part load conditions. The compressor only undergoes cycling losses at D condition when the required operating frequency to match the heating load is below minimum possible compressor frequency of 15 Hz. The compressor can match the heating load at C condition because of the reduced $T_{weg,co,out}$ and pressure ratio. The $SCOP_{avg}$ for this compressor at these conditions is 5.47.

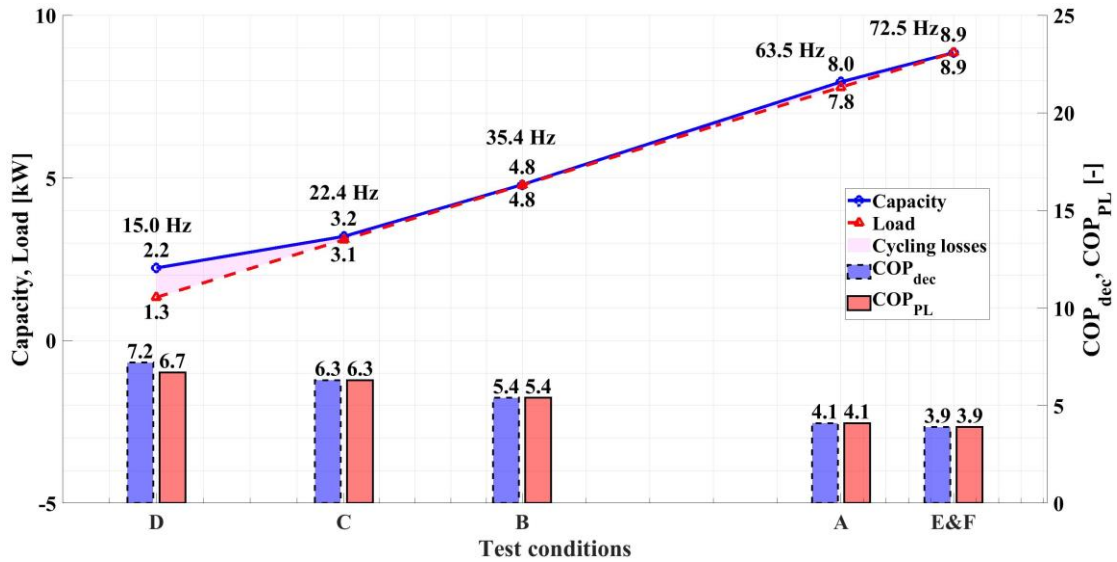


Fig. 9. Seasonal performance of variable speed compressor with variable $T_{weg,co,out}$

4.4. Comparison of $SCOP_{avg}$ for all the investigated cases

The $SCOP_{avg}$ values calculated using the $COP_{PL,avg}$ for all the different tested cases are shown in Table 5. The case 4 with 1.25 kg of refrigerant charge and variable $T_{weg,co,out}$ is 26.3% higher than the case 1 with 1.5 kg of refrigerant charge and fixed $T_{weg,co,out}$. The $SCOP_{avg}$ of the compressor when tested according to the variable $T_{weg,co,out}$ is 21.5% higher than when tested according to constant $T_{weg,co,out}$ with 1.50 kg of charge and it is 21.0% with 1.25 kg of charge. This higher $SCOP_{avg}$ is due to the lower $T_{weg,co,out}$ which causes a drop in the compressor operating pressure and power consumption. Additionally, the compressor can match the heating capacity during the variable $T_{weg,co,out}$ test cases at the C condition and operate at the minimum possible frequency at the D condition. This eliminates the cycling losses at the C condition and reduces the cycling losses at D condition. These lead to a higher $COP_{PL,avg}$ for the case with variable $T_{weg,co,out}$. The $SCOP_{avg}$ for case 2 with fixed $T_{weg,co,out}$ and lower charge is 5.3% than the equivalent case 1 with higher refrigerant charge. Similar improvement of 4.8% is observed when comparing cases 3 and 4 with the variable $T_{weg,co,out}$. These difference cases show that there is an effect of test standard as well as the refrigerant charge on the seasonal performance estimates and the impact of test standard is significantly higher.

Table 5 $SCOP$ estimates for all the cases investigated

Case #	Charge [kg]	Fixed/Variable Condenser WEG outlet	$SCOP_{avg}$ [-]	Difference in $SCOP_{avg}$ [%]	$\dot{Q}_{co+sc,avg}$ at full load condition [kW]	Difference in full load $\dot{Q}_{co+sc,avg}$ [%]
1	1.50	Fixed	4.33	-	9.08	-
2	1.25	Fixed	4.56	+5.3%	8.85	-2.5%
3	1.50	Variable	5.26	+21.5%	9.08	-
4	1.25	Variable	5.47	+26.3%	8.85	-2.5%

5. Conclusions

This study experimentally studied the effect of charge and the fixed/variable outlet condition on the seasonal performance of an R410A water heat pump with a variable speed compressor. The $SCOP_{avg}$ for the variable speed compressor with variable outlet condition was 21.5% higher than the fixed outlet condition. The variable speed compressor cannot match the required heating load at one of the part load conditions with fixed outlet condition due to the required pressure ratio being outside the compressor operating envelop. This problem does not occur for the variable outlet condition, and this leads to a lower cycling losses and higher $SCOP_{avg}$.

Charge optimization for the variable speed compressor was done at part load conditions and a peak in $COP_{dec,weg}$ was observed at a charge before the receiver starts filling up. This maximum $COP_{dec,weg}$ occurs due to the relative amounts of heat transfer happening in the condenser and subcooler and the optimum charge corresponds to the scenario when some portion of the two phase heat transfer is happening in the subcooler. The peak in $COP_{dec,weg}$ is due to the interaction between the increase in power consumption due to reduced two phase heat transfer area in the subcooler and the increased heating capacity due to higher subcooling in the subcooler. The relative difference between these two factors causes a peak in $COP_{dec,weg}$. When the variable speed compressor was operated at this optimum charge, the $SCOP_{avg}$ improved by 5.3% for the fixed outlet condition and 4.8% for the variable outlet condition. Thus, the COP_{dec} can improve if the system is operated in region 2.

However, the heating capacity at the full load drops by around 2% when operating at lower refrigerant charge. Any refrigerant leak in the system can also move the operating charge to region 1 which drops the COP_{dec} significantly. So, it is recommended to operate the system in region 3 to get a higher COP_{dec} but not a huge drop in heating capacity. Additionally, operating a dedicated subcooler system with a receiver installed in between the condenser and subcooler at the peak COP_{dec} does not make use of the installed receiver and the maximum possible subcooling from the dedicated subcooler.

Nomenclature

BPHX	braze plate heat exchanger [-]	Subscripts	
C_d	degradation coefficient [-]	1-phase	single phase refrigerant
COP	coefficient of performance [-]	2-phase	two phase refrigerant
CR	capacity ratio [-]	avg	average
c_p	specific heat [kJ/kg]	co	condenser
EXV	electronic expansion valve [-]	cp	compressor
GWP	global warming potential [-]	dec	declared
h	enthalpy [kJ/kg]	ev	evaporator
$IPLV.SI$	integrated part load value [-]	in	inlet
LMTD	log mean temperature difference [K]	load	required heating load
m	mass flow rate [g/s]	out	outlet
p	pressure [kPa]	PL	part load
Q	heat transfer rate [kW]	ref	refrigerant
$SCOP$	seasonal coefficient of performance [-]	ri	refrigerant inlet
T	temperature [°C]	ro	refrigerant outlet
UA	overall heat transfer coefficient [kW/K]	sc	subcooler/subcooling
W	power [W]	sc+co	subcooler and condenser
WEG	water ethylene glycol [-]	sh	superheat
x	refrigerant quality [-]	weg	water ethylene glycol

Greek
symbols

Δ difference [%]
 ε error [%]

Acknowledgements

The authors would like to thank the member companies of the Air Conditioning and Refrigeration Center at the University of Illinois at Urbana-Champaign for their funding to support this project, Emerson / Copeland for compressor samples, Danfoss for brazed plate heat exchangers, and Creative Thermal Solutions for the technical support.

References

- [1] Kim, W., & Braun, J. E., 2012. Evaluation of the impacts of refrigerant charge on air conditioner and heat pump performance. *International journal of refrigeration*, 35(7), 1805-1814.
- [2] Goswami, D. Y., Ek, G., Leung, M., Jotshi, C. K., Sherif, S. A., & Colacino, F., 2001. Effect of refrigerant charge on the performance of air conditioning systems. *International journal of energy research*, 25(8), 741-750.
- [3] Inampudi S.T., Elbel S., 2022, "Study of charge optimization and compressor modulation strategies effect on the seasonal performance in a R410A chiller," 19th International Refrigeration and Air Conditioning Conference at Purdue, West Lafayette, IN, USA, July 11 -14, Paper 1199
- [4] Inampudi S., Elbel S., 2022, "Experimental investigation into the effect of charge optimization and compressor modulation strategies on the seasonal performance in a R410A chiller," 16th International Conference on Heat Transfer, Fluid Mechanics and Thermodynamics - HEFAT 2022, Amsterdam, The Netherlands, August 08-10, Paper 131
- [5] European Committee for Standardization, 2013. Standard EN 14825: 2013, Air conditioners, liquid chilling packages and heat pumps with electrically driven compressors for space heating and cooling. Testing and rating at part load conditions and calculation of seasonal performance.
- [6] Inampudi S.T., Botticella F., Elbel S., 2021, "Experimental comparison of seasonal performance in R410A chiller using single speed and two stage compressor," 18th International Refrigeration and Air Conditioning Conference at Purdue, West Lafayette, IN, USA, May 23-28, Paper 1484
- [7] Inampudi S., Botticella F., Elbel S., 2021, "Part load performance of single and two stage compressors – a comparative experimental study in a R410A chiller unit," 12th International Conference on Compressors and their Systems, London, UK, September 6-8, Paper 184
- [8] Inampudi S.T., Botticella F., Elbel S., 2022, "Comparative experimental analysis of different compressor capacity modulation strategies in R410A chiller with focus on seasonal performance," 19th International Refrigeration and Air Conditioning Conference at Purdue, West Lafayette, IN, USA, July 11 -14, Paper 1198
- [9] Lemmon, E. W., Bell, I. H., Huber, M. L., & McLinden, M. O., 2018. NIST Standard Reference Database 23: Reference Fluid Thermodynamic and Transport Properties-REFPROP, Version 10.0, National Institute of Standards and Technology. Standard Reference Data Program, Gaithersburg
- [10] A. H. R. I., 2020. AHRI Standard 551/591 (SI): 2020 Standard for performance rating of water-chilling and heat pump water-heating packages using the vapor compression cycle. Air-Conditioning, Heating, Refrigeration Institute, Arlington, VA, USA.
- [11] Sieres, J., Ortega, I., Cerdeira, F., Álvarez, E., & Santos, J. M., 2022. Seasonal Efficiency of a Brine-to-Water Heat Pump with Different Control Options according to Ecodesign Standards. *Clean Technologies*, 4(2), 542-554.